17th World Conference on Earthquake Engineering, 17WCEE

Sendai, Japan - September 13th to 18th 2020

SEISMIC PERFORMANCE OF RAILWAY BRIDGE MASONRY PIERS RETROFITTED WITH GRID-STEEL PLATE SYSTEM

Ngoc T. PHAN[(1)], Akira. HOSODA[(2)], Hamed. SALEM[(3)], A.I. ZERIN[(4)], S. TAKAHASHI[(5)], N. SASAKI[(6)]

(1) Graduate student, Graduate School of Urban Innovation, Yokohama National University, phan-ngoc-ms@ynu.jp
(2) Professor, Institute of Urban Innovation, Yokohama National University, concrete@ynu.ac.jp
(3) Professor, Structural Engineering Department, Cairo University, Egypt, hhadhoud@appliedscienceint.com
(4) Post-Doctoral Researcher, Institute of Urban Innovation, Yokohama National University, Japan, email: zerin-iffat-nj@ynu.jp
(5) Engineer, Structural Engineering Center, East Japan Railway Company, email: saki-takahashi@jreast.co.jp
(6) Manager, Structural Engineering Center, East Japan Railway Company, email: naomi-sasaki@jreast.co.jp

Abstract

More than sixty unreinforced brick masonry old railway bridges are still in service in Kanto metropolitan area in Japan which are vulnerable to seismic damages. According to past history, several brick masonry bridges were collapsed at the events of the Nobi Earthquake (1891), the Great Kanto Earthquake (1923), the Fukui Earthquake (1948), the Miyagi-ken Earthquake (1978), the Central Japan Sea Earthquake (1983) and the Niigata Earthquake (2004) interrupting consistent railway communications. Hence, appropriate retrofitting techniques are indispensable to maintain the serviceability of existing old masonry railway bridges in Japan. In order to enhance the performance of unreinforced masonry piers in very limited spaces under severe seismic actions, grid-steel plate retrofitting system has been developed. The philosophy of this method is to prevent the large horizontal sliding and residual displacement at the mortar joints between bricklayers which may cause catastrophic failure of structures or difficulty of early resuming railway service after the earthquake. The rocking behavior instead of sliding of bricklayers in the retrofitted pier is desired to perform in this developed system under seismic actions. At the final step, to give sufficient seismic performance for the whole bridge system, stoppers to restrict the displacement of piers and abutments will be attached to the upper girders to prevent the piers from falling or overturning. In this research, the effectiveness of the grid-steel plate retrofitting system was confirmed through a set of experiments. There were four cases of testing specimens including separated concrete blocks which were joined by grid-steel plate system with different details. The grid-steel plate retrofitting system showed a good contribution to minimize the sliding behavior of the retrofitted column at the joint and caused rocking behavior at the base of the specimens in both cases of two and three separated concrete blocks. Furthermore, the details of grid-steel plate retrofitting method were improved through the lessons from four specimens to prevent unexpected cracking and local failure in concrete blocks and the rupture of the horizontal penetrating steel bars connecting steel plates. Applied Element Method (AEM) was used to simulate the structural performances of the specimens, and sufficient modeling techniques and calibrated parameters were also obtained. It is concluded that the AEM simulation is reliable as a numerical analysis method for analyzing the important influencing factors when the grid-steel plate system will be applied to the brick specimens.

Keywords: Applied Element Method (AEM); grid-steel plate retrofitting system; masonry piers; seismic performance

1. Introduction

More than sixty unreinforced brick masonry old railway bridges are still in service in Kanto metropolitan area in Japan which are vulnerable to seismic damages. According to past history, several brick masonry bridges were collapsed at the events of the Nobi Earthquake (1891), the Great Kanto Earthquake (1923), the Fukui Earthquake (1948), the Miyagi-ken Earthquake (1978), the Central Japan Sea Earthquake (1983) and the Niigata Earthquake (2004) interrupting consistent railway communications, as shown in Fig. 1 [1]. Hence, appropriate retrofitting techniques are indispensable to maintain the serviceability of existing old masonry railway bridges in Japan. The investigation of past earthquake damage cases done by Structure Design Office, Japan National Railways in 1987 [1, 2] pointed out that the characteristics of the damage are the horizontal sliding and large residual displacement of bricklayers at the mortar joints (Fig. 1). Moreover, the space around many existing masonry railway bridge piers is very limited. Therefore, in many cases, the jacketing method which is the most common seismic rehabilitation technique proposed by Ishibashi et al. is difficult to apply [3]. A research given by Tadokoro et al. proposed the partial steel plate retrofitting method for strengthening brick masonry piers using steel plates covering the side surfaces and the steel plates would be anchored to the footing through welded steel bars. The retrofitted pier became a composite structure consisting of compressive-resistant masonry and tensile-resistant steel plates [4].

In this research, a new method named grid-steel plate retrofitting method, which is different from the method by Tadokoro, et al. will be developed. This method is aimed to prevent sliding at the joints and spalling of brick blocks and is not aimed to increase the capacity of piers. At the first step of the development, separated concrete blocks are retrofitted by the newly developed grid-steel plate retrofitting method and static cyclic loading was conducted. Numerical simulations by the Applied Element Method were conducted and verified by the experimental results.

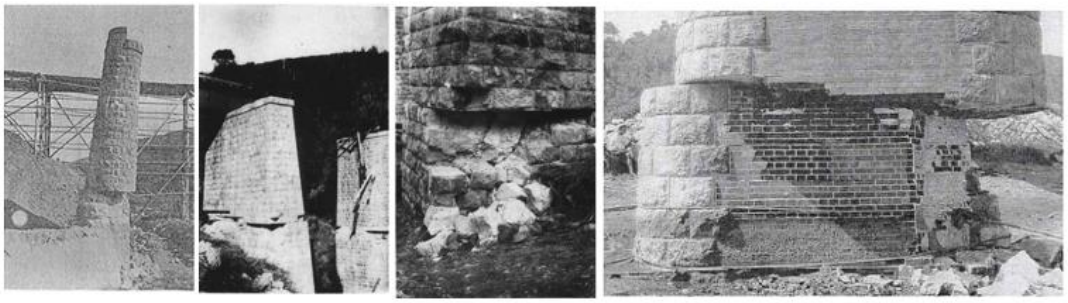

Fig.1 – Damage of unreinforced masonry railway structures under big earthquakes

2. Grid-steel plate retrofitting method

2.1 The philosophy of the Grid-steel plate retrofitting method

As mentioned in the introduction, the failure mode of the unreinforced masonry piers became horizontal sliding of the bricklayers and large residual displacement at the mortar joints which may cause catastrophic failure of structures or difficulty of early resuming railway service after earthquakes. Therefore, the grids of thin steel plates that are connected by penetrated steel bars are proposed to cover the side surfaces of the brick pier for enhancing its seismic performance (Fig. 2). The philosophy of the retrofitting system using grid-steel plate system is to mitigate the large residual displacement and horizontal sliding at the mortar joints of bricklayers. The retrofitted brick piers are expected to rock at the base instead of sliding between bricklayers under seismic actions. Consequently, to give sufficient seismic performance for the whole bridge system, stoppers to restrict the displacement of piers and abutments will be attached to the upper girders to prevent the piers from falling or overturning, as shown in Fig. 3.

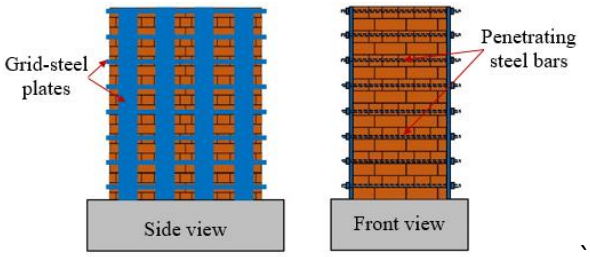

Fig. 2 – The Grid-steel plate retrofitting method

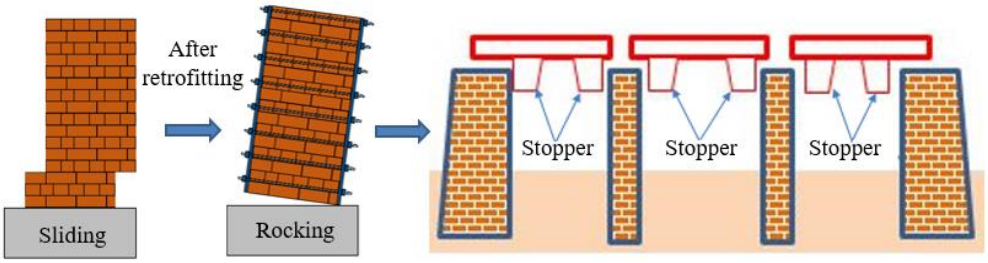

Fig. 3 – The philosophy of the Grid-steel plate retrofitting method

2.2 The setting details of laboratory test

During the earthquake, the brick pier will be horizontally separated into independent parts due to the complete failure of horizontal mortar layers connecting bricklayers. Sliding between those parts is resisted only by the friction of the sliding surfaces. Therefore, in order to economically check the effectiveness of the grid-steel plate system, concrete blocks representing for separated parts of the brick pier were reasonably utilized. The objective of the testes is to confirm the details of the grid-steel plate system in which the rocking behavior can be obtained as the failure mode.

2.1.1 The details of specimens

There were four cases of testing specimens including separated concrete blocks joined by grid-steel plate system. For Case 1, Case 2 and Case 3, the specimens were composed of two-separated concrete blocks named upper block and lower block, as shown in Fig. 4. For Case 4, the specimen was composed of three-separated concrete blocks named upper block, middle block and lower block, as shown in Fig. 5. The grid-steel plate system includes pairs of steel plate SS400 connected by horizontal penetrating steel bars SR235. A polyvinyl chloride (PVC) sheet was located at the joint of concrete blocks representing the worst case when very small friction is generated at the sliding surfaces in reality. In the experiment, the friction between PVC sheet and concrete blocks at the surface of the joint is the main factor causing sliding at the joint. The use of PVC sheet was to drastically reduce the block friction and to investigate the contribution of the grid-steel system. The friction behavior between PVC sheet and concrete blocks in the experiments must be much weaker than that of the joint in actual structures. Therefore, it is reasonable to conclude that with the same grid-steel plate retrofitting system, the sliding at the joint in real structures must be prevented. The upper block was subjected to horizontal and axial loading through corresponding loading systems while the lower block was placed on the hardened RC footing through a construction joint where the top surface of the footing was made rough. The footing was fixed to the concrete floor through anchor bolts.

In the laboratory test series, the later cases were improved learning from the previous case resulting in the alternation of the height *(H)* of the 600x600mm concrete blocks, the alternation of width *(b)*, length *(l)*, thickness *(t)*, the arrangement of the grid-steel plate system, and the number of concrete blocks, as shown in Table 1 and Table 2. The interface material between steel plates and concrete column was also investigated.

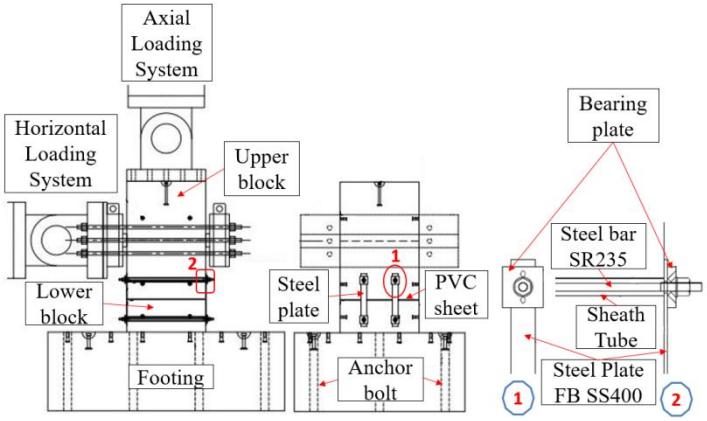

Fig. 4 – The details of specimens for Case 1, 2, 3

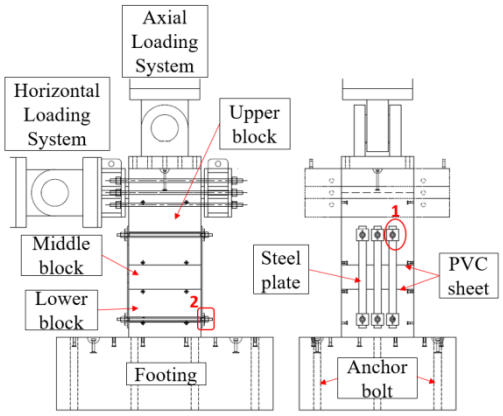

Fig. 5 – The details of specimens for Case 4

Table 1 – Details of columns and PVC sheet

Case	Upper column			Middle column			Lower column			PVC sheet
	Height *(H)*	Width *(b)*	Length *(l)*	Height *(H)*	Width *(b)*	Length *(l)*	Height *(H)*	Width *(b)*	Length *(l)*	Thickness *(t)*
	(mm)	(mm)	(mm)	(mm)	(mm)	(mm)	(mm)	(mm)	(mm)	(mm)
1	1150	600	600	-			250	600	600	4
2	900	600	600				250	600	600	4
3	900	600	600				500	600	600	0.5
4	800	600	600	200	600	600	400	600	600	0.5

Table 2 – Details of steel plates, bearing plates, sheath tubes and steel bars

Case	Steel plate FB SS400			Bearing plate			Sheath tube	Rebar SR235
	$t \times b \times h$ (mm)			$t \times b \times h$ (mm)			ϕ (mm)	ϕ (mm)
1	3	32	240	12	50	50	20	9
2	1.6	45	400	12	60	60	30	11
3	9	72	860	25	120	120	50	23
4	9	72	860	25	120	120	50	23

2.1.2 The material properties

The material properties of concrete and steel used in the experiments are illustrated in Table 3 and Table 4.

Table 3 – Characteristics of concrete

Case	Concrete column		Concrete footing	
	average compressive strength	average tensile strength	average compressive strength	average tensile strength
	(N/mm^2)	(N/mm^2)	(N/mm^2)	(N/mm^2)
1	19.4	2.98	29.9	3.76
2	42.1	4.42	43.6	4.41
3	46.0	3.4	42.9	4.51
4	43.3	3.82	43.6	4.18

Table 4 – Characteristics of steel

Case	Steel plate SS400		Steel bar SR 235	
	yield stress	yield strain	yield stress	yield strain
	(N/mm^2)	(μ)	(N/mm^2)	(μ)
1	379	1761	361	1723
2	329	1525	1104	7097
3	304	1460	1014	4886
4	304	1460	998	4970

2.3 The development of grid-steel plate retrofitting system through experimental series

2.2.1 Test results of Case 1

In Case 1, the grid-steel plate retrofitting system included three pairs of 3mm thickness steel plate connected with 9mm diameter of penetrating steel bars. The specimen was subjected to only horizontal-controlled displacement without axial loading. After cyclic horizontal displacements of ±1mm, ±7mm, ±13mm were applied to the upper block, the monotonic loading was continued until failure (Fig. 6a). The test was stopped when a horizontal penetrating steel bar was ruptured at the intersection with the steel plate, as shown in Fig. 6c. The lower concrete block showed severe diagonal cracks at its both top edges starting from the horizontal penetrating steel bar to the top surface (Fig. 6b). Fig. 7 illustrates that those diagonal cracks were reasonably explained as punching shear failure due to the insufficient shear fracture surface which is defined as the distance from the center of horizontal penetrating steel bar to the top of lower concrete block.

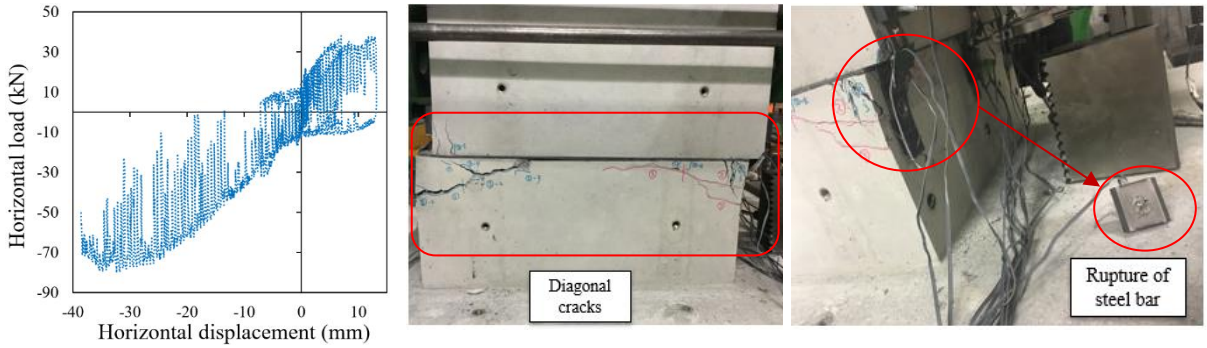

a) Load-displacement relationship b) Punching shear failure c) Rupture of horizontal steel bar

Fig. 6 – Performance of Case 1 specimen

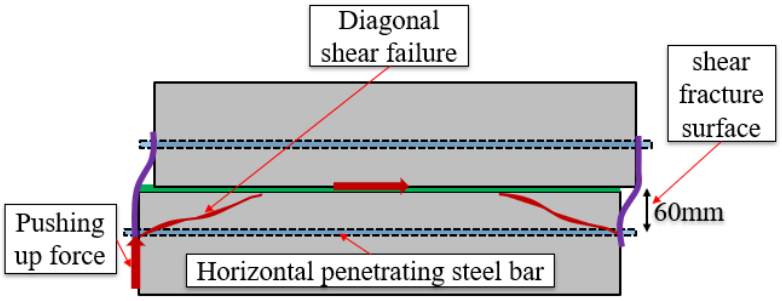

Fig. 7 – Punching shear failure at lower concrete block

2.2.2 Test results of Case 2

The grid-steel plate retrofitting system in Case 1 showed unexpected damages of the lower concrete block and failure of the horizontal penetrating steel bar which did not satisfy the requirement for easy restoration of the retrofitted member after the earthquakes. Therefore, in Case 2, the shear fracture surface was increased from 60mm to 150mm (Fig. 9). In addition, only two pairs of steel plate were provided whose thickness was reduced from 3mm to 1.6mm while the diameter of the horizontal penetrating steel bars was increased from 9mm to 11mm. This modified retrofitting system was expected to prevent the diagonal cracks in concrete blocks and not to in connecting steel bars but to fail in steel plates. Moreover, the epoxy resin added in between steel plates and the concrete column surface in Case 1 was replaced by spongy pads of 60x60x6mm in Case 2. The spongy pads created a gap of 3mm from steel plates to concrete surfaces for minimizing the undesirable high stress concentration due to contacts during initial stages of horizontal loading.

The specimen was subjected to 0.1N/mm^2 axial compression which was evenly distributed on the top of the upper concrete block. Then, cyclic horizontal-controlled displacement of ±2mm, ±5mm were given. After that, monotonic horizontal loading was applied to the upper block until failure (Fig. 8a). The failure happened in the steel plates at the intersection with horizontal steel bars, as shown in Fig. 8c. It was confirmed that there was no punching shear failure at the lower concrete block and no breakage of horizontal steel bars. However, a severe vertical crack causing spalling in lower concrete block was found (Fig. 8b). Based on the observation during the monotonic horizontal loading, the elongation of steel plates became larger allowing rocking of the upper block. The combination of sliding and eccentric compression caused cracking and spalling concrete in the lower block, as shown in Fig. 9. Moreover, there were some unexpected protrusions of the PVC sheet during cyclic horizontal loading that caused early contact between PVC sheet and steel plates. This unexpected contact produced additional tension in steel plates.

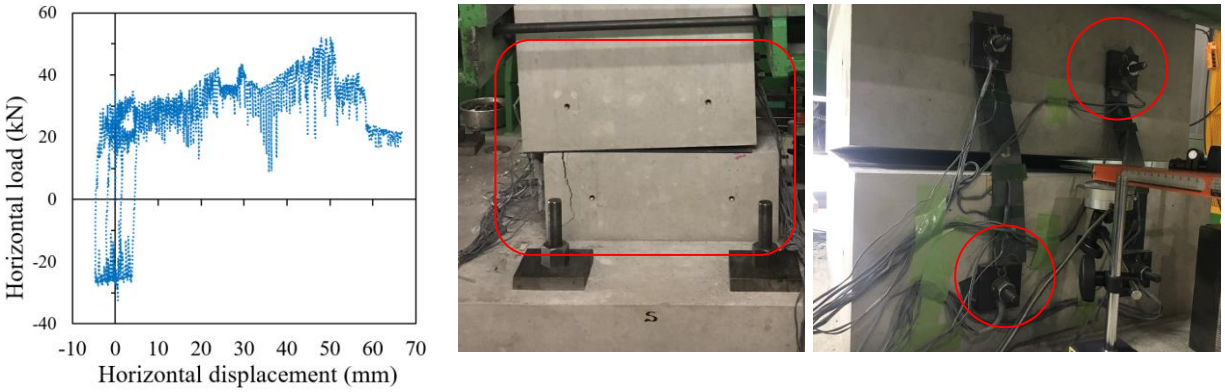

a) Load-displacement relationship b) Cracking in lower block c) Rupture of horizontal steel bar

Fig. 8 – Performance of Case 2 specimen

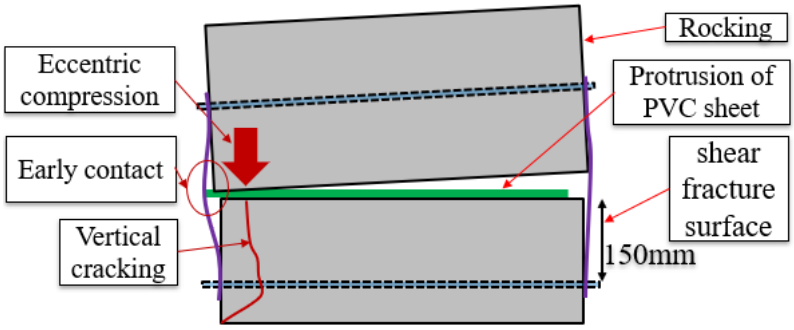

Fig. 9 – Cracking in lower concrete block

2.2.3 Test results of Case 3

Although the failure of Case 2 specimen happened in the steel plate in a desirable way, the rocking behavior was not observed at the base. Therefore, in Case 3, the thickness of the steel plates was greatly increased to 9mm and three pairs of steel plates were applied to connect the concrete blocks. The unexpected early contact between steel plates and PVC sheet was tried to be eliminated by using a soft PVC sheet of 0.5 mm thickness. Moreover, larger spongy pads of 120x120x12mm were added to prevent local failure between steel plates and concrete blocks.

The same axial compressive stress was given to the specimen as in Case 2. After that, cyclic horizontal-controlled displacements of ±6mm, ±12mm, ± 18mm, ±24mm, ±27mm, ±30mm were applied, and after that monotonic horizontal loading was continued till failure (Fig. 10a). During the monotonic horizontal loading, the rocking behavior was observed at the base of the retrofitted column with a significant

decrease of the loading capacity while a relative horizontal sliding of 16mm was observed between upper and lower block (Fig. 10b, 10c). There was no severe crack in concrete column and the maximum strain in the steel plates reached their yielding strength.

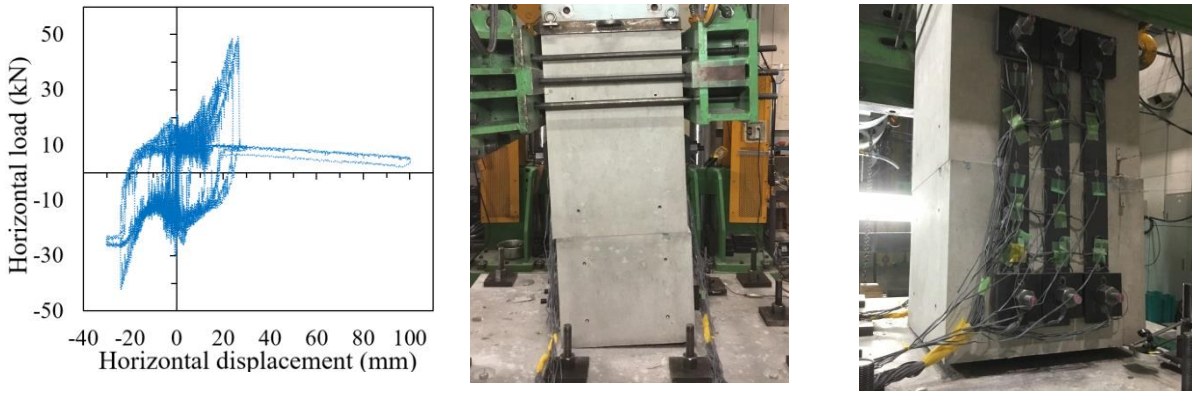

a) Load-displacement relationship b) Rocking behavior (front view) c) Rocking behavior (side view)

Fig. 10 – Performance of Case 3 specimen

2.2.4 Test results of Case 4

In Case 4, the same details of the grid-steel plate system of Case 3 were used by which rocking behavior of the retrofitted column were confirmed. The tested column included three separated concrete blocks representing for the possible severe failure condition when brick piers subjected to big earthquakes, as shown in Fig. 11b.

The loading procedure included evenly distributed 0.1N/mm^2 axial compression, cyclic horizontal-controlled displacements of ±4mm, ±6mm, ±12mm, ±18mm, ±24mm, ±30mm, ±36mm and monotonic horizontal loading until failure (Fig. 11a). During the cyclic horizontal loading the middle block showed relative horizontal displacements both to upper and lower blocks. The retrofitted column showed rocking behavior at the base without failure of steel plate system and severe crack in concrete blocks (Fig. 11b, 11c).

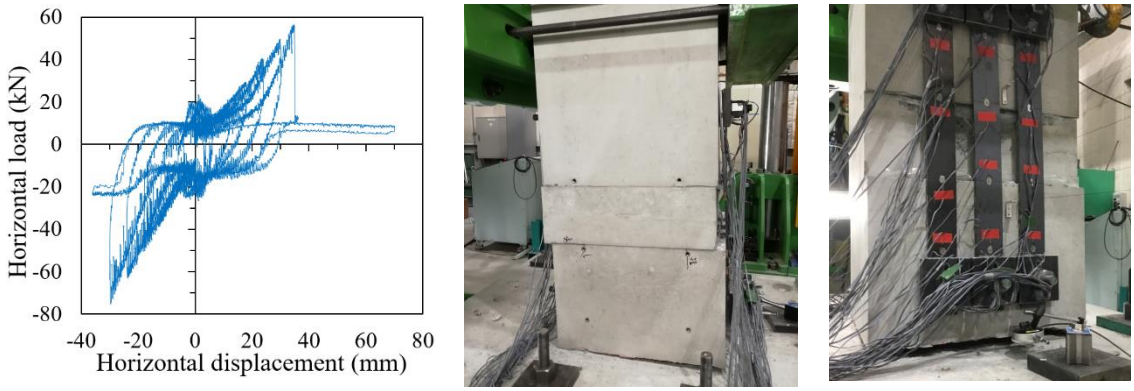

a) Load-displacement relationship b) Rocking behavior (front view) c) Rocking behavior (side view)

Fig. 11 – Performance of Case 4 specimen

3. Simulation verification following Applied Element Method (AEM)

3.1 Applied Element Method (AEM)

The AEM is a developed numerical analysis method which was initially developed at the University of Tokyo in 1998 by Meguro and Tagel-Din [5] adopting the concept of discrete cracking. In AEM, structures

are modeled as an assembly of small elements. The elements are connected using their whole surfaces through a set of normal and shear springs. Each spring represents stresses, strain, deformations of a certain volume of the material [7], as shown in Fig. 12. Each two adjacent elements can be totally separated once the springs connecting them are ruptured. This method, therefore, can reliably follow the cracking initiation and propagation, and load deformation of the structural behavior from the initial stages until complete collapse [8, 9]. Fully nonlinear path-dependent constitutive models are adopted in AEM. When concrete is subjected to compression, elasto-plastic and fracture model of Maekawa and Okamura 1983 are adopted [10]. For concrete in tension, linear stress-strain relationship is adopted until cracking of concrete springs, where the stresses drop to zero. As for steel material, the reinforcing bars are modeled as bare bars for the envelope [11] while the model represented by Ristic et al. is used for interior loops [12].

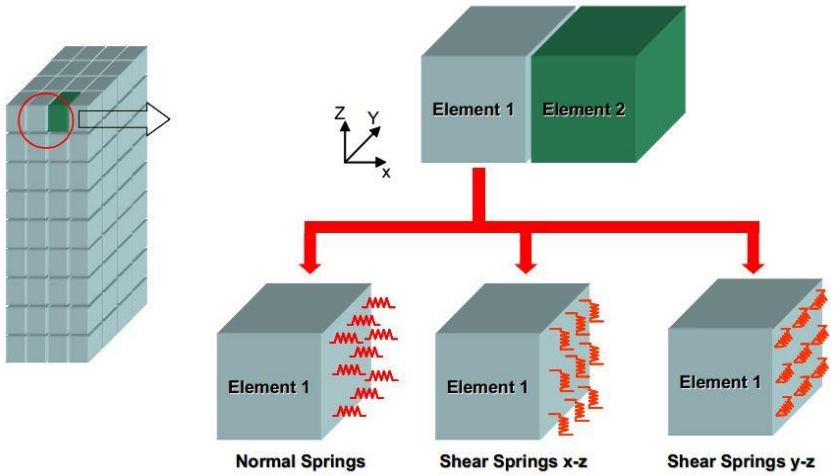

Fig. 12 – Connectivity matrix spring in AEM

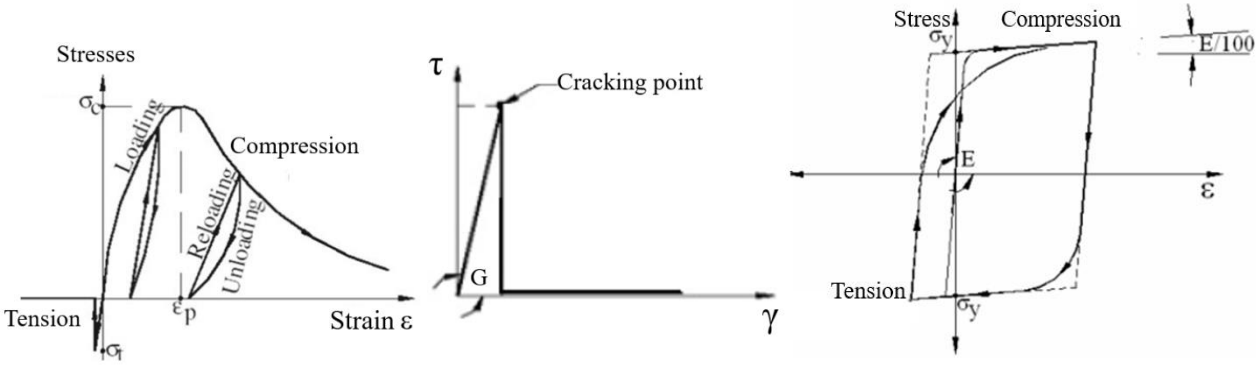

a) Concrete under axial stress and shear stress b) Reinforcement under axial stress

Fig. 13 – Constitutive models for concrete and reinforcement

In AEM, an interface material model is used for modeling the springs connecting two rigid bodies with different material types. The bearing interface material model is a pre-cracked model in which the material is initially cracked and cannot carry tensile stresses. In compression, the stress-strain relationship is assumed linear up to compression failure stress. The shear stress-strain relationship is linear till the shear stress exceeds $\mu\sigma_n$ (coefficient of friction times normal stress) [13]. When a material is assumed elastic, the stress-strain ratio is continuously constant, and the stresses and strains can reach very high values without any changes in the material behavior [11].

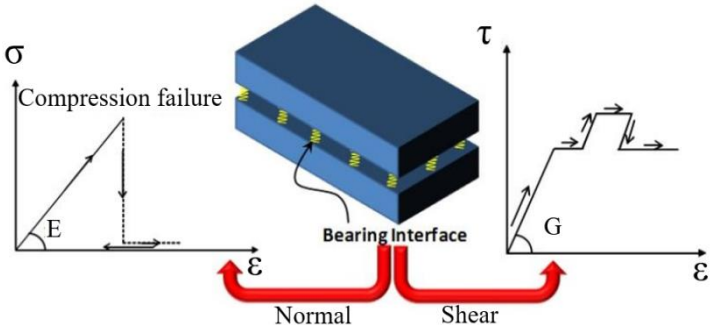

Fig. 14 – Constitutive models for bearing material

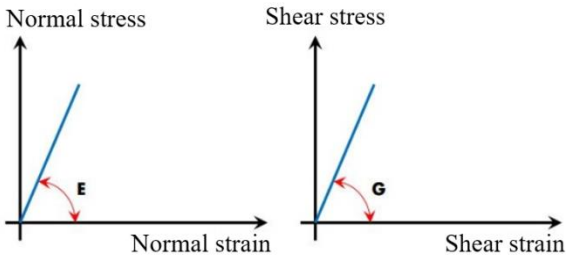

Fig. 15 – Constitutive models for elastic material

3.2 Influencing factors in AEM modeling

The loading capacity of the retrofitted specimens was mainly governed by the strength of the grid-steel plates system, the sliding friction between concrete blocks and the inserted PVC sheet, the amount of applied loading and the tensile strength of the construction joint between the lower block and the footing. Moreover, the contacts between steel plates and concrete surfaces also caused some undesirable high stress concentrations in the initial stages of cyclic horizontal loading.

In AEM simulation, the important influencing parameters above were calibrated in monotonic analysis. After that, the models with calibrated parameters were used for cyclic analysis and the simulation results were verified by the experimental results. The observation and data from the tests such as the load-displacement relationship, cracks generated in concrete blocks, and failure mode of the grid-steel plate system were fully utilized for the verification.

3.2.1 Interface material between concrete blocks and PVC sheet

In the experiment, the PVC sheet was inserted into the joint between separated concrete blocks without bonding. Therefore, their interface material in AEM model should be only active for transferring axial compressive stresses, and shear stiffness and shear stress will be small during horizontal sliding. The bearing material explained in section 3.1 was reasonably adopted to model the interface material between concrete blocks and PVC sheet, as shown in Fig. 16. The small friction at this interface was obtained by calibrating appropriate values for shear modulus (G) and friction coefficient (μ) of the bearing interface material.

Due to the unexpected protrusion of the PVC sheet with 4mm thickness in Case 2 (which was also used in Case 1) causing early stress development in the steel plates, the thickness of PVC sheet was reduced to 0.5mm in Case 3 and Case 4. Hence, the shear modulus (G) and friction coefficient (μ) were changed for two kinds of PVC sheets. From the calibration results, it was confirmed that the bearing interface material with μ=0.2 and G=5N/mm^2 were reliable for Case 1 and Case 2 while in Case 3 and Case 4, the bearing interface material with μ=0.1 and G=0.1N/mm^2 were reasonable.

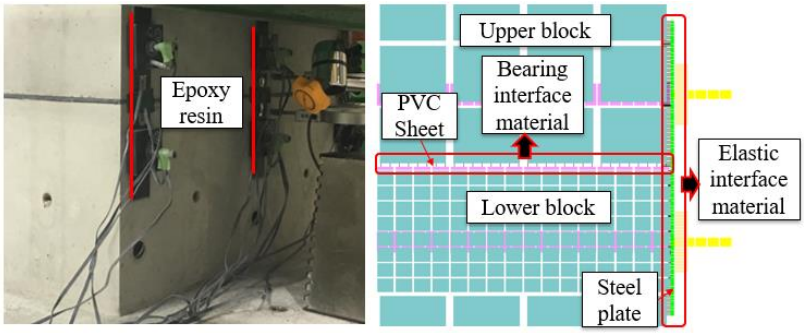

Fig. 16 – Interface material Case 1

3.2.2 Interface material between concrete column and steel plates

The bond strength of steel plates and concrete surface connected by epoxy resin in Case 1 was not measured. In AEM simulation, the elastic material explained in section 3.1 was adopted for the interface material between steel plates and concrete surface as shown in Fig. 16. The calibration results showed that the elastic interface material with Young's modulus of 100N/mm^2 and separation strain of 1.0 was appropriate.

3.2.3 Modeling for spongy pads

An elastic material with Young's modulus of 100N/mm^2 modeling the spongy pads was used which could create corresponding gaps between steel plates and concrete surface in Case 2, Case 3 and Case 4 (Fig. 17).

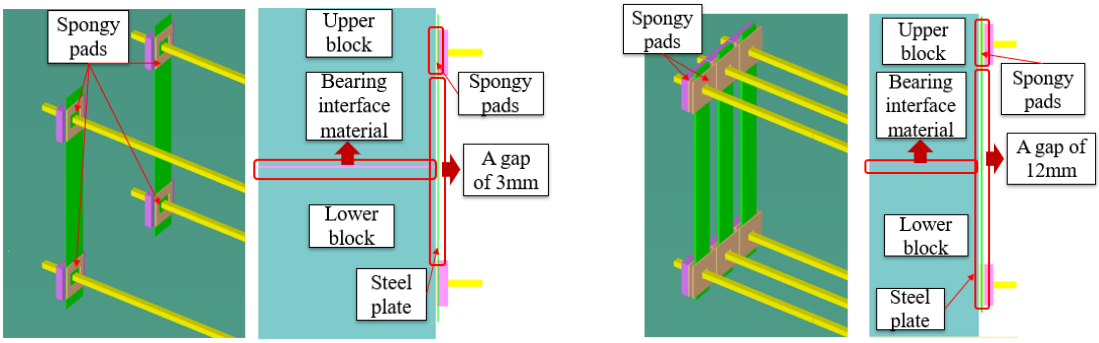

a) Case 2 b) Case 3

Fig. 17 – Modeling of spongy pads

3.2.4 Interface material for construction joint between lower concrete block and footing

As mentioned in section 2.1.1, the lower concrete block was connected to the footing through a construction joint. The tensile strength of the joint was not measured in the experiment. In AEM models, the calibration results showed that the concrete interface material with tensile strength of 1.5N/mm^2 was reliable to simulate the cracking load at the construction joint.

3.3 Verification of AEM models

The influencing factors governing the AEM simulation results of the specimens in this research were fully calibrated and verified by experimental results in the past research [1]. Fig. 18, Fig. 19 and Fig. 20 show reliable agreements in terms of horizontal load-displacement relationship, the cracking generated in the concrete block, the failure of the grid-steel plate system and compatible rocking behavior.

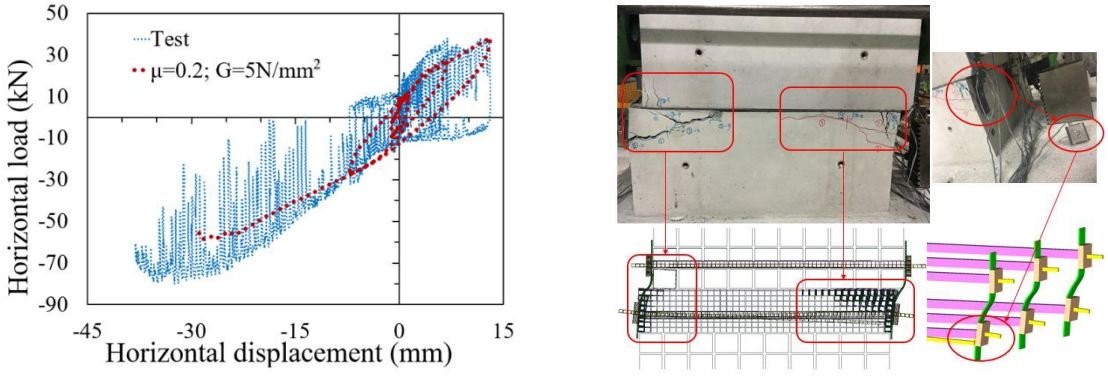

a) Load-displacement relationship b) Cracking and failure mode in AEM simulation

Fig. 18 – AEM simulation for Case 1

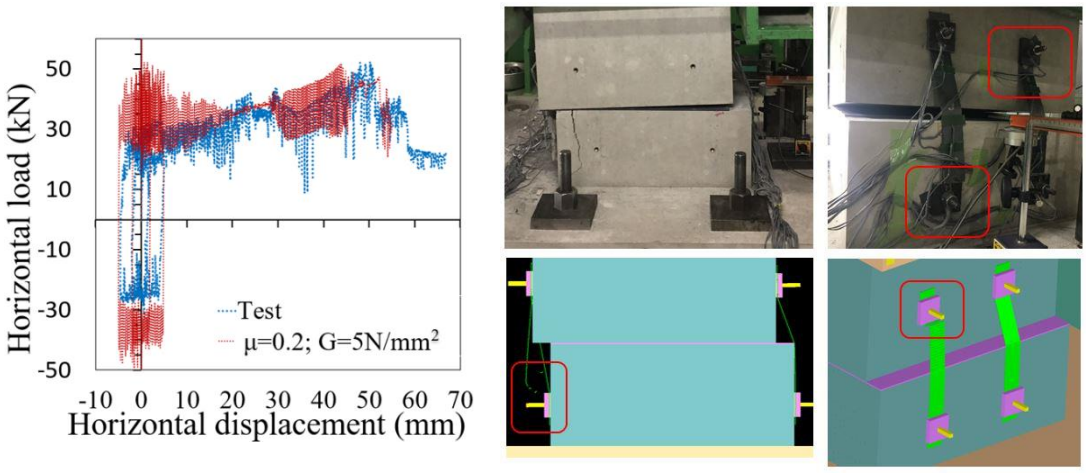

a) Load-displacement relationship b) Failure mode in AEM simulation

Fig. 19 – AEM simulation for Case 2

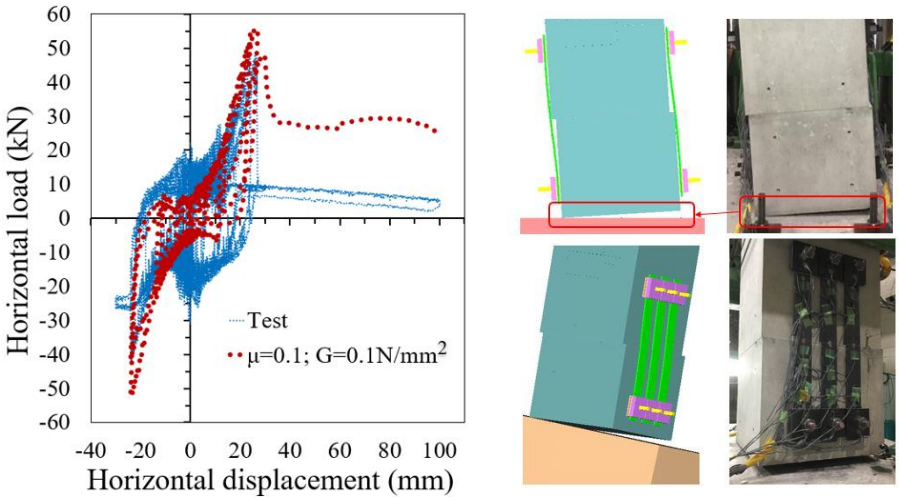

a) Load-displacement relationship b) Rocking behavior

Fig. 20 – AEM simulation for Case 3

4. Conclusions

A new seismic retrofitting method for a masonry piers or abutments of bridges, grid-steel plate system was developed. The efficiency of this new method was verified in experiment, and the structural performances of the retrofitted specimens were numerically simulated by Applied Element Method, the following conclusions could be drawn:

(1) The grid-steel plate retrofitting system was successfully verified to contribute to minimize the sliding behavior of the retrofitted column at the joint and caused rocking behavior at the base of the specimens in both cases of two and three separated concrete blocks.

(2) The details of grid-steel plate retrofitting method were improved learning from experimental series to prevent unexpected cracking and local failure in concrete blocks and the rupture of the horizontal penetrating steel bars connecting steel plates.

(3) The AEM simulation is reliable as a numerical simulation method for analyzing the important influential factors when the grid-steel plate system is applied to the brick specimens and to masonry specimens.

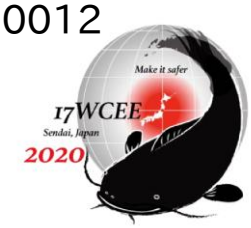

References

[1] Japan National Railways (1987): Guideline for repair and retrofit of masonry and plain concrete structures. *Structure Design Office* (in Japanese).

[2] Watanabe Kazuaki et. al. (2006): A study on the earthquake resistance of stone or brick piers. *Taisei Construction Technology Center Bulletin* (in Japanese), **39**.

[3] Ishibashi, T., Tsuyoshi, T. and Kobayashi, K (2004): Seismic retrofitting methods newly developed for railway concrete structures. *Journal of Advanced Concrete Technology*, **2**(1), 65-76.

[4] Tadokoro, T., Tottori, S., Hattori, H. (2005): Experiment and Finite Element Analysis for Flexural and Shear Behavior of Masonry Piers. *RTRI REPORT*, **19**(12), 39-44.

[5] Tagel-Din, H., and Meguro, K. (2000a): Applied element method for dynamic large deformation analysis of structures. *Struct. Eng. Earthquake. Eng., JSCE,* **17**(2), 215–224.

[6] Tagel-Din, H., and Meguro, K. (2000b): Applied element method for simulation of nonlinear materials: Theory and application for RC structures. *Struct. Eng. Earthquake Eng., JSCE*, **17**(2), 123s–148s.

[7] Meguro, K. and Tagel-Din, H. S. (2002): Applied element method used for large displacement structural analysis. *Journal of Natural Disaster Science*, **24**(1), 25-34.

[8] Meguro, K. and Tagel-Din, H. S. (2000): Applied element method for dynamic large deformation analysis of structures. *Doboku Gakkai Ronbunshu*, **17**(661), 1-10.

[9] Helmy, H., Salem, H. and Mourad, S. (2012): Computer-aided assessment of progressive collapse of reinforced concrete structures according to GSA code. *Journal of Performance of Constructed Facilities*, **27**(5), 529-539.

[10] Maekawa, K. and Okamura, H. (1983): The deformational Behavior and Constitutive Equation of Concrete using the Elasto-plastic and Fracture Model", *Journal of the Faculty of Engineering, The University of Tokyo*, **37**(2), 253-328.

[11] International, A.S.: p. LLC (ASI) www.appliedscienceint.com

[12] Ristic, D., Yamada, Y. and Iemura, H. (1986): Stress-Strain Based Modeling of Hysteretic Structures under Earthquake Induced Bending and Varying Axial Loads. *Research report No. 86-ST-01*, School of Civil Engineering, Kyoto University, Kyoto, Japan.

[13] Salem, H., Mohssen, K., Kosa, K. and Hosoda, A. (2014): Collapse analysis of Utatsu Ohashi bridge damaged by Tohuku tsunami using applied element method, *Journal of Advanced Concrete Technology*, **12**(10), 388-402.

[14] Ngoc T. P., Hosoda, A., Salem, H, Takahashi, S. (2019): AEM analysis of grid-steel plate retrofitting method for masonry piers of railway bridges, *CI Annual convention in Sapporo, Japan,* **41**(2), 1291-1296.

